J. Anat. (1997) **190**, pp. 377–395, with 20 figures Printed in Great Britain

Spermiogenesis and spermiation in a marsupial, the tammar wallaby (*Macropus eugenii*)

MINJIE LIN, AMANDA HARMAN AND JOHN C. RODGER

Co-operative Research Centre for Conservation and Management of Marsupials, Department of Biological Sciences, University of Newcastle, NSW, Australia

(*Accepted 5 November 1996*)

ABSTRACT

Fourteen steps of spermatid development in the tammar wallaby (*Macropus eugenii*), from the newly formed spermatid to the release of the spermatozoon into the lumen of the seminiferous tubules, were recognised at the ultrastructural level using transmission and scanning electron microscopy. This study confirmed that although the main events are generally similar, the process of the differentiation of the spermatid in marsupials is notably different and relatively more complex than that in most studied eutherian mammals and birds. For example, the sperm head rotated twice in the late stage of spermiogenesis: the shape of the spermatid changed from a T-shape at step 10 into a streamlined shape in step 14, and then back to T-shape in the testicular spermatozoa. Some unique figures occurring during the spermiogenesis in other marsupial species, such as the presence of Sertoli cell spurs, the nuclear ring and the subacrosomal space, were also found in the tammar wallaby. However, an important new finding of this study was the development of the postacrosome complex (PAC), a special structure that was first evident as a line of electron dense material on the nuclear membrane of the step 7 spermatid. Subsequently it became a discontinuous line of electron particles, and migrated from the ventral side of the nucleus to the area just behind the posterior end of the acrosome, which was closely located to the sperm–egg fusion site proposed for *Monodelphis domestica* (Taggart et al. 1993). The PAC and its possible role in both American and Australian marsupials requires detailed examination. Distinct immature features were discovered in the wallaby testicular spermatozoa. A scoop shape of the acrosome was found on the testicular spermatozoa of the tammar wallaby, which was completely different to the compact button shape of acrosome in ejaculated spermatozoa. The fibre network found beneath the cytoplasm membrane of the midpiece of the ejaculated sperm also did not occur in the testicular spermatozoa, although the structure of the principle piece was fully formed and had no obvious morphological difference from that of the epididymal and ejaculated spermatozoa. The time frame of the formation of morphologically mature spermatozoa in the epididymis of the tammar wallaby needs to be determined by further studies.

Key words: Marsupial spermiogenesis; spermatogenesis; spermatids; testicular spermatozoa; acrosome; tammar wallaby.

INTRODUCTION

Spermiogenesis, the remarkable morphological and biochemical transformation of the round spermatid into the elongate spermatozoon, is one of the most complex cell differentiations found in animals. During this process of spermatozoon formation the spermatid reduces its cell volume more than a hundred times, radically changes its shape and produces a number of morphologically elaborate organelles, including the acrosome, the midpiece and the flagellum. The biochemical transformation of the spermatid is equally complex. During this period the proteins of the unique cytoskeletal elements of the spermatozoon (e.g. perinuclear theca, outer dense fibres and fibrous sheath) are synthesised; these have little resemblance

Correspondence to Dr Minjie Lin, Department of Biological Sciences, University of Newcastle, NSW 2308, Australia. Fax: 61-49-216923; Email: biml@cc.newcastle.edu.au.

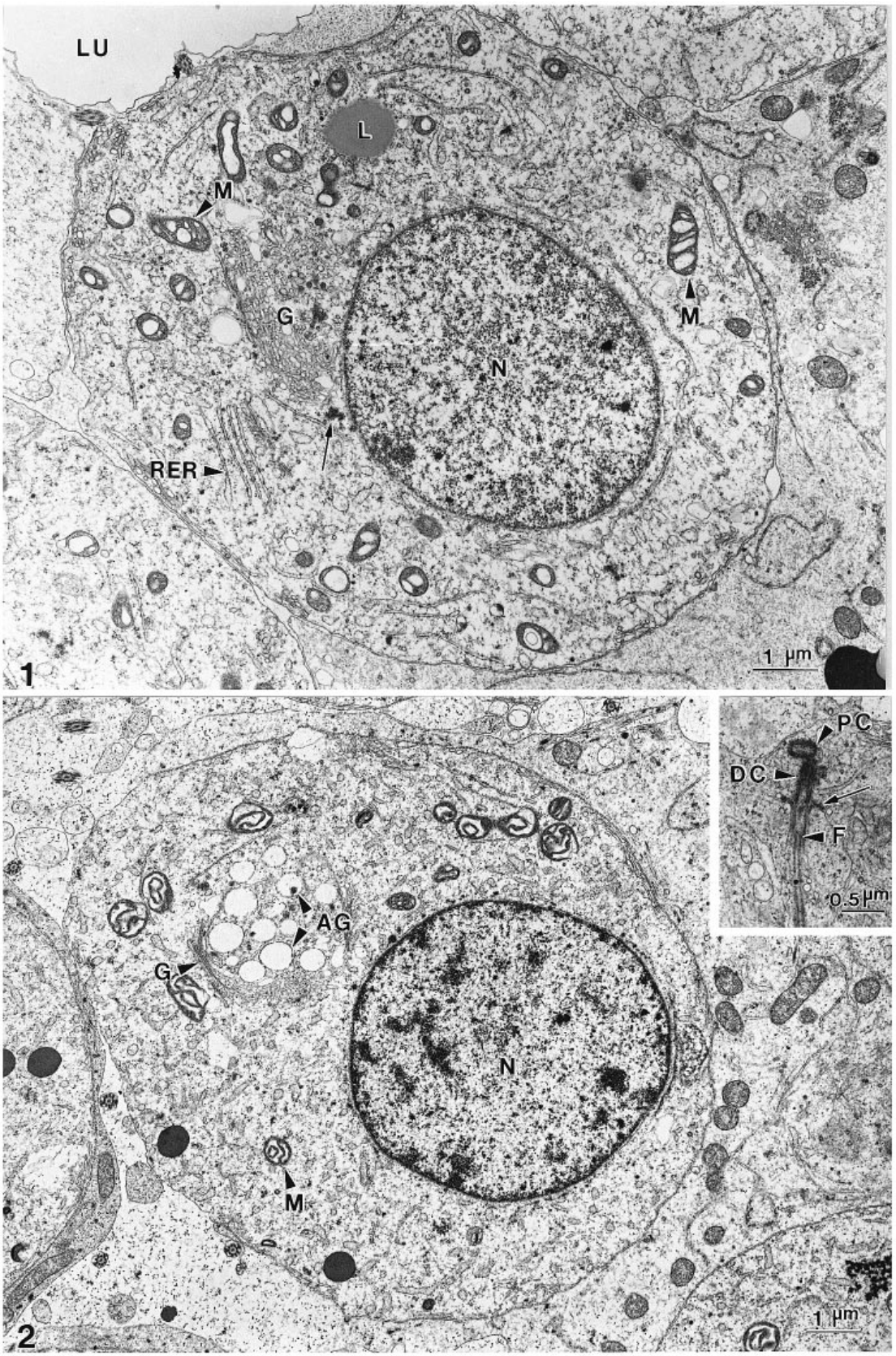

Fig. 1. Electron micrograph showing a step 1 spermatid of the tammar wallaby. The spermatid, located on the top layer of the seminiferous epithelium, possesses a round nucleus (N) with homologous chromatin. Golgi bodies (G) and centrioles (arrow) are seen. Mitochondria (M) with large spaces between their cristae, and rough endoplasmic reticulum (RER) are scattered throughout the cytoplasm. LU, lumen of the seminiferous tubule; L, lipid droplet.

to cytoskeletal proteins of somatic cells. Some genes that control the synthesis of these sperm proteins are expressed only in the spermatid and only during spermiogenesis (Oko, 1995). The differentiation of spermatids has attracted extensive investigation, not only because the differentiation involves many radical changes in the shape and biochemistry of the spermatid, but because the phases or steps in spermiogenesis have provided a basis for analysing the spermatogenic cycle of the seminiferous epithelium. A good deal of information on spermiogenesis has been accumulated for mammals and birds (reviewed in Setchell, 1978; Guraya, 1987; Jones & Lin, 1993; Lin & Jones, 1993).

In marsupials the main morphological events of spermiogenesis are generally similar to those described for eutherian mammals, involving formation of the acrosome, transformation of the shape of the nucleus, elimination of cytoplasm and configuration of the flagellum (reviewed in Harding et al. 1979, 1982; Temple-Smith, 1987; Bedford, 1991). However, marsupial spermatids show a variety of unique structural changes during their differentiation which give the sperm head a distinct dorsal and ventral character. Thus (1) the acrosome is positioned asymmetrically on the dorsal face of the head; (2) the tail is inserted into a fossa in the midventral surface of the nucleus; and (3) the nucleus rotates through variable degrees to form a T configuration between the nucleus and the tail (Bedford, 1991). All these features are due to the manner of nuclear flattening which in marsupials is at 90° to the forming tail rather than parallel to the tail as in eutherians (Rodger, 1991). These unique morphological characters add additional complications in the investigation of the formation of some organelles and structures during spermiogenesis in marsupials. The release of the spermatozoon from the seminiferous epithelium, spermiation, has not been described for any marsupial at the ultrastructural level.

Studies of the ultrastructural differentiation of the marsupial spermatid are limited to relatively few species; honey possum (*Tarsipes rostratus*) (Harding et al. 1984), common brushtail possum (*Trichosurus vulpecula*) (Harding et al. 1976), woolly opossum (*Caluromys philander*) (Phillips, 1970), long-nosed bandicoot (*Perameles nasuta*) (Sapsford et al. 1967, 1969*a*, *b*) and some dasyurids (Harding et al. 1982). Most of these studies include only general observations on spermiogenesis because the primary interest was in posttesticular maturation events in the epididymis. Description of spermiogenesis is either not given in detail or restricted to certain stages in the process of sperm differentiation. Classification of spermiogenesis into consecutive stages (9 stages) has been done for only one marsupial, the allied rock wallaby (*Petrogale assimilis*) (Kim et al. 1987).

The present study describes spermiogenesis and spermiation in the tammar wallaby (*Macropus eugenii*) at the ultrastructural level using transmission and scanning electron microscopy. Fourteen steps of spermatid development were recognised, from the newly formed spermatid to the release of the spermatozoon into the lumen of the seminiferous tubules. The study aimed to provide a basis for more detailed studies of male gamete formation and extratesticular maturation in marsupials using the tammar wallaby as a model species.

MATERIALS AND METHODS

Three adult male tammar wallabies (*Macropus eugenii*) were obtained from Kangaroo Island in South Australia and maintained in the breeding yard of the Marsupial Co-operative Research Centre at the University of Newcastle, New South Wales, Australia. These animals had all been used as semen donors in other experiments and were thus known to have recently produced ejaculates containing large numbers of highly motile spermatozoa. The animals were killed with an overdose of sodium pentobarbitone (30 mg/kg, intravenously) via a lateral tail vein. The use of protected animals and animal experimentation were approved by the appropriate state authorities and by the Animal Care and Ethics Committee of the University of Newcastle, respectively.

Testes were dissected and fixed in 2.5% (v/v) glutaraldehyde and 2% paraformaldehyde in 0.1 cacodylate buffer for 4 h at room temperature (RT), or overnight at 4 °C. The tissues were postfixed in 1% osmium tetroxide for 1 h. After dehydration through a series of concentrations of acetone, the tissues were embedded in Spurr's resin (Agar Scientific Ltd, Essex, UK). Sections (70–100 nm) were cut on an Ultracut E ultramicrotome (Reichert-Jung, Austria) with a dia-

Fig. 2. Electron micrograph of a step 2 spermatid of the tammar wallaby. The chromatin in the nucleus is condensed into patches. Several membrane-bound vesicles (AG) are associated with Golgi bodies (G). The proximal centriole (PC) and the distal centriole (DC) are oriented at a right angle to each other (see inset). The distal centriole protrudes from the cell body to form the flagellum (F) of the sperm. The precursor of the annulus of the tail (arrow) appears as a ring of electron dense material along the inner cytoplasmic membrane on the base of the flagellum. M, mitochondria.

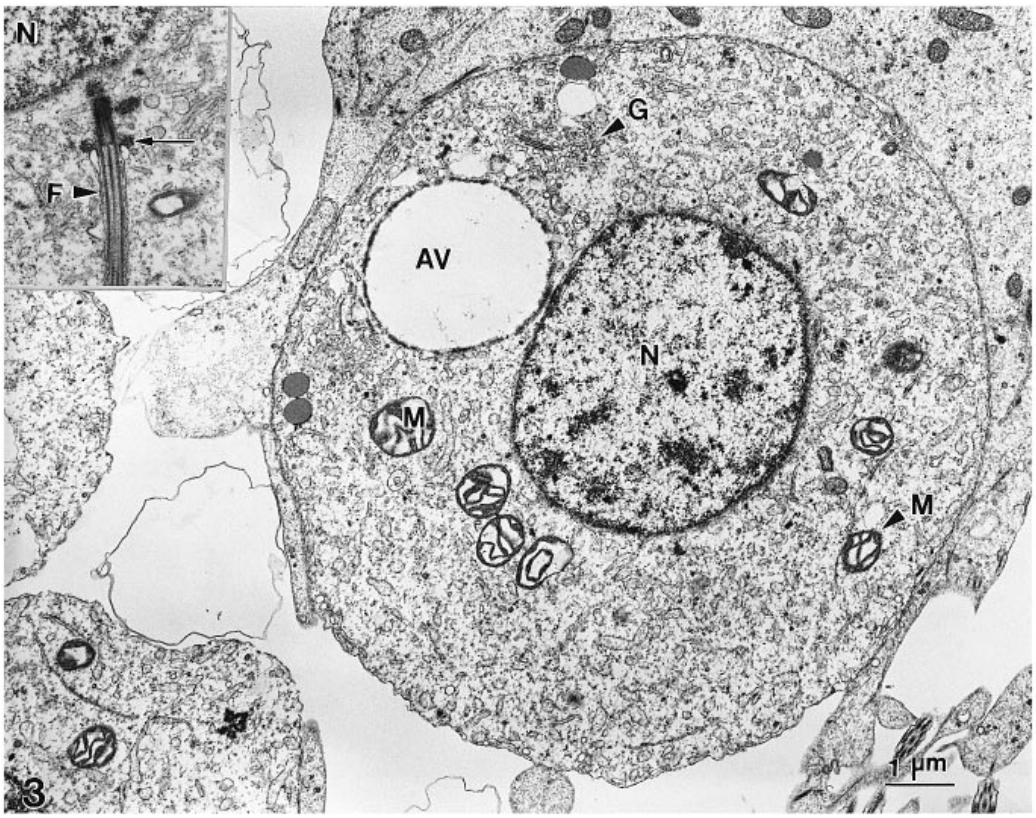

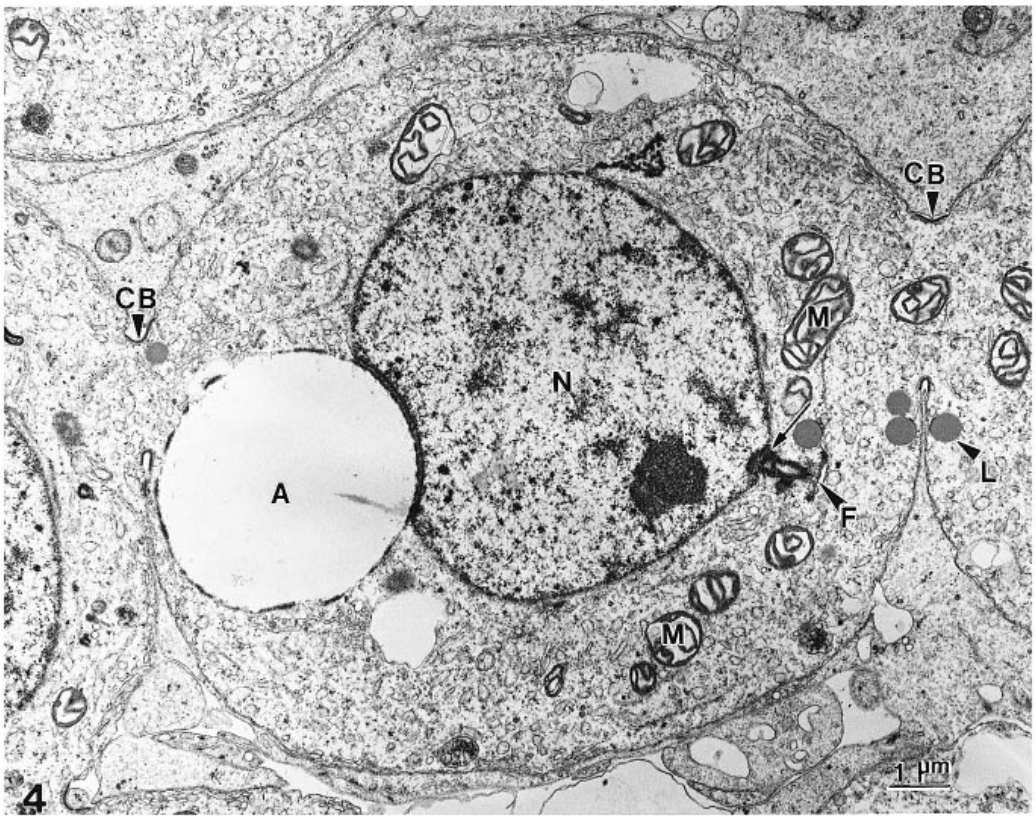

Fig. 3. Electron micrograph of a step 3 spermatid of the tammar wallaby. A large acrosomal vacuole (AV) with a rather transparent appearance has been formed, adjoining the nuclear membrane, after gradually approaching the nucleus (N). The inset shows that a concavity on the surface of the nucleus (N) is forming to accommodate the flagellum (F). More amorphous material is attached to the electron dense ring of the formative annulus (arrow). G, Golgi bodies; M, mitochondria.

Fig. 4. Electron micrograph of a step 4 spermatid of the tammar wallaby. The acrosome (A) is lodged into a concavity of the nuclear membrane. Membranes of the acrosome and the nucleus (N) along the contact site are intensely stained. The flagellum (F) has migrated to the pole of the nucleus opposite the acrosome and is fully lodged into the concavity on the surface of the nucleus (arrow). The spermatids are connected to each other by cytoplasmic bridges (CB). M, mitochondria; L, lipid droplet.

mond knife (Diatome Ltd, Bienne, Switzerland), and then stained with 1% uranyl acetate in 30% (v/v) ethanol (Watson, 1958) for 5–10 min, followed by lead citrate for 10–20 min. Micrographs were taken by a JEOL-100CX transmission electron microscope (JEOL, Tokyo, Japan) operating at 80 kV.

Specimens for scanning electron microscopy were initially prepared using the same fixation procedures as above, except that the tissues were fixed overnight at 4 °C. They were then treated with 1% osmium tetroxide for 4 h at RT. After processing through the dehydration and the critical point drying, the tissues were coated with gold and examined in a JSM 840 scanning electron microscope (JEOL, Tokyo, Japan) operated at 15 kV.

For light microscopy, testis tissues were fixed and processed into Spurr's resin using the same procedure as above. Sections (1.0–1.5 μm) were cut with glass knives and stained with a solution containing 1% (w/v) toluidine blue and 0.5% (w/v) borax in 30% (v/v) ethanol. Micrographs were taken by a Zeiss Axiophot microscope (Zeiss, West Germany).

RESULTS

Spermiogenesis

Spermatid differentiation was classified into 14 steps based on the morphological development of the acrosome, the shaping of the nucleus and formation of the flagellum. In line with normal practice for marsupial spermatozoa the term dorsal is used to refer to the acrosomal surface of the head (Cleland, 1956) and ventral relates to the surface where the flagellum is inserted (Cleland & Rothschild, 1959; Hughes, 1965).

Step 1 spermatids (*Fig. 1*). Step 1 spermatids were roughly spherical in shape and usually located in the top layers of the seminiferous epithelium adjacent to the lumen. The nuclei were round and contained fine granular chromatin spread evenly throughout the nucleoplasm. A conspicuous Golgi body was usually located next to the nucleus and, adjacent to the Golgi body, a pair of centrioles destined to form the flagellum of the spermatozoon. Rough endoplasmic reticulum and mitochondria with large spaces between their cristae were scattered throughout the cytoplasm. A small number of lipid droplets were present in the cytoplasm.

Step 2 spermatids (*Fig. 2*). The nuclei remained spherical with a narrow band of flocculent chromatin beneath the nuclear membrane and condensed patches of chromatin throughout the nucleoplasm. Membrane-bound secretory vesicles which contained patches of electron-dense material were associated with the Golgi bodies. The 2 centrioles were oriented to each other at a right angle. The proximal centriole was shorter and located closer to the nucleus. The distal centriole was elongated, and protruded from the cell to form the flagellum (see insert, Fig. 2). The formative flagellum possessed only axonemal tubules in the 9 + 2 pattern. A ring of electron-dense material, the precursor of the annulus, was closely associated with the posterior centriole (Fig. 2, insert). This electron dense materials occurred on the inner surface of the cytoplasmic membrane where the flagellum projected from the cell body. Other cell organelles were similar to those in step 1 spermatids.

Step 3 spermatids (*Fig. 3*). Nuclear shape and appearance were similar to those of step 2 spermatids. The numerous secretory vesicles evident in step 2 were now fused into a single large acrosomal vacuole adjacent to the nucleus. Only a thin band of dense material was attached to the inner membrane of the acrosomal vacuole. Some dispersed fibre-like material was also visible within the acrosomal vacuole but a definitive acrosomal granule such as seen in eutherian mammals (Bloom & Fawcett, 1975) was never present (see Fig. 3). The flagellum protruded further from the cell body than in step 2 spermatids. The formative annulus became more obvious at the base of the invagination of the plasmalemma around the axoneme. While the formative flagellum stretched further way from the cell body, its base (the proximal centriole) became located close to the nucleus. A concavity on the surface of the nucleus had begun to form to accommodate the proximal centriole. Coincidentally, the developing flagellum and acrosome migrated towards their final locations at the opposite poles of the nucleus. Other organelles in the cytoplasm were similar to those in the step 2 spermatids.

Step 4 spermatids (*Fig. 4*). The shape of step 4 spermatids remained roughly spherical. Within the nuclei the chromatin was further condensed into large patches. The acrosome reached its maximum size and was lodged into a depression on the surface of the nucleus. Both membranes along the contact site of the acrosome and the nucleus were thickened and electron dense. The acrosome had an empty appearance with only a very small amount of dispersed material around the periphery. A discontinuous narrow band of electron-dense material lay along the acrosomal membrane. The proximal centriole, the base of the flagellum, was now fully lodged into the concavity of the nuclear membrane (see Fig. 4). The flagellum and acrosome were now close to their final locations on

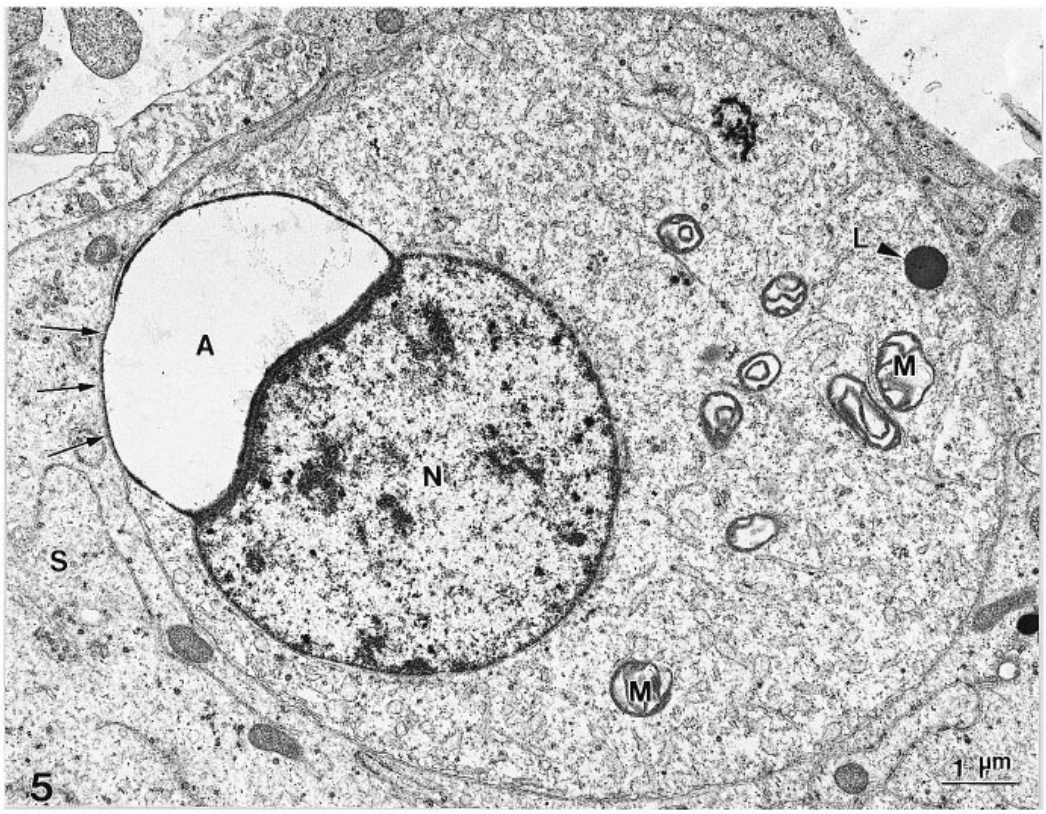

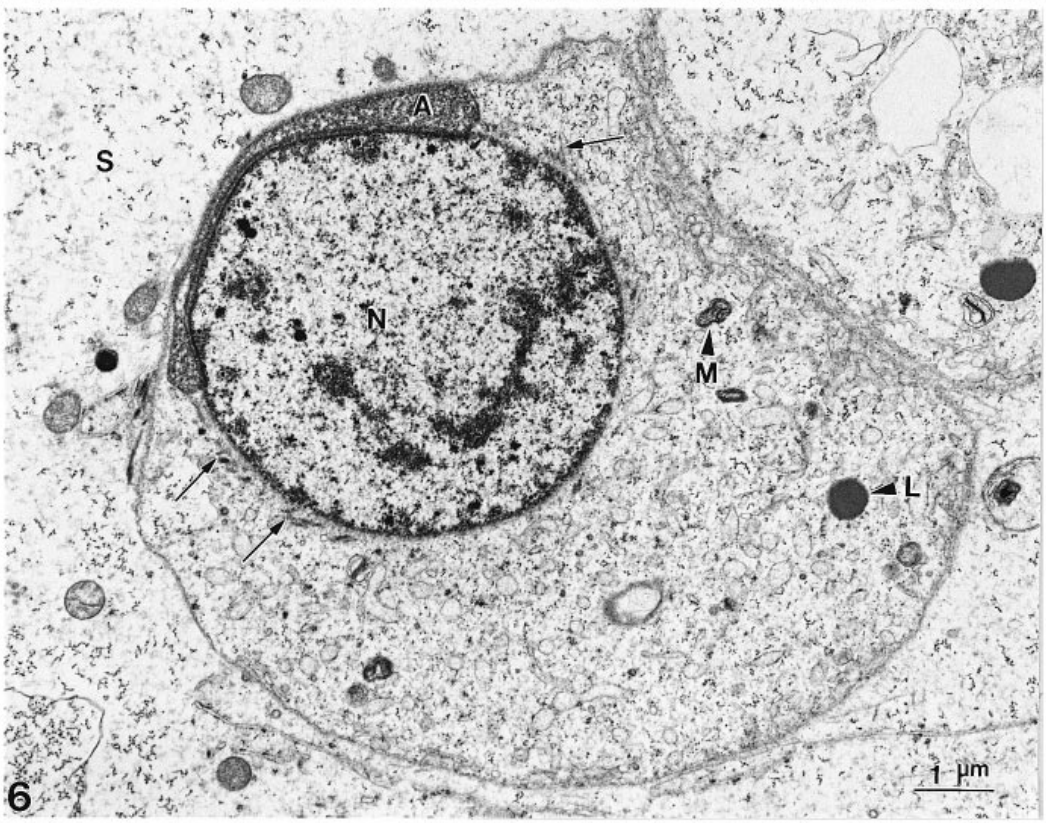

Fig. 5. Electron micrograph of a step 5 spermatid of the tammar wallaby. The acrosome (A) is ellipsoidal and has an empty appearance. Membranes between the acrosome and the nucleus (N) are thickened by the accumulation of electron-dense material. The rostral surface of the acrosome contacts the plasma membrane (arrows) of the spermatid. S, cytoplasm of Sertoli cells; M, mitochondria; L, lipid droplet.
Fig. 6. Electron micrograph of a step 6 spermatid of the tammar wallaby. The acrosome (A) contains granular material and covers almost one-third of the nuclear surface. Some microtubules (arrows), precursors of the manchette, appear on the lateral sides of the nucleus (N). M, mitochondria; L, lipid droplet; S, cytoplasm of Sertoli cells.

opposite sides of the nucleus. Other organelles were similar to those in step 3 spermatids.

Step 5 spermatids (*Fig. 5*). The nuclei remained roughly spherical and contained heterogeneous chromatin. At this stage the acrosome still had an empty appearance and contained only sparse filamentous material. The acrosome was now no longer spherical, but covered nearly one third of the surface of the nucleus and its rostral surface was in contact with the plasma membrane. A conspicuous electron-dense deposit was associated with the region of the acrosomal membrane in contact with the nucleus. However, the area of acrosomal membrane in contact with the spermatid plasma membrane lacked the electron-dense deposit.

Step 6 spermatids (*Fig. 6*). The nuclei remained heterochromatic with condensed chromatin patches. The acrosome had condensed into a narrow cap like structure which covered one-third of the nuclear surface. The acrosome was no longer empty in appearance but filled with a granular matrix. Microtubules of the manchette first appeared near the lateral surface of the nucleus and adjacent to the acrosome. Microtubules were absent from the future ventral pole of the nucleus opposite the acrosome. At step 6, spermatids had begun to lose their spherical shape and the cytoplasm migrated to the caudal end of the cell.

Step 7 spermatids (*Fig. 7*). Step 7 was a period of major change. The nucleus appeared to protrude from the cell due to the caudal migration of the cytoplasm. Although still roughly round in shape the nucleus had begun to undergo marked chromatin decondensation into homogenous granules. The condensed chromatin granules were evenly distributed throughout the nucleus except for an electron lucent area beneath the nuclear membrane between the forming nuclear ring and neck socket. This region of the nucleus eventually became the posterior ventral side of the sperm head. The nuclear membrane adjacent to this electron lucent area and near the neck socket was characterised by a conspicuous accumulation of electron-dense granules (see Fig. 7). This special structure was designated the postacrosomal complex, since it migrated with the shifting nuclear membrane and was ultimately located at the posterior end of the acrosome in mature spermatids (see Figs 13, 14). The acrosome was a narrow homogenous layer which covered the whole anterior end of the nucleus. In addition to the postacrosomal complex, 2 other unique structures of the marsupial spermatid were first seen in step 7 spermatids adjacent to the boundary of the acrosome. The nuclear ring first appeared as a band of dense material on the inner surface of the plasma membrane of the spermatid. The Sertoli cell spurs (Sapsford et al. 1967) appeared as a band of electron-dense material in the Sertoli cell cytoplasm (see Fig. 7, and insert). The microtubules of the manchette were present in the thin band of cytoplasm surrounding the nucleus, distal to the nuclear ring. The base of the flagellum had migrated near to its final destination, the neck socket (Sapsford et al. 1967), which was formed by the thickening and invagination of the nuclear membrane, at the pole of the nucleus opposite the acrosome.

Step 8 spermatids (*Fig. 8*). Dorsal–ventral flattening of the spermatid nucleus commenced at this step and the nuclei took on a roughly square shape. As a result the attached acrosome had a flattened appearance. Despite this further condensation of the nucleus, the electron lucent area adjacent to the postacrosomal complex persisted. The Sertoli cell spurs and the nuclear ring continued to grow and became more obvious. The attachment between the tail and the head of the spermatids was established as the flagellum made contact with the nuclear socket. The annulus became more prominent as a result of further accumulation of electron dense material.

Step 9 spermatids (*Fig. 9*). The nuclei of step 9 spermatids had an asymmetric appearance. The electron lucent area within the nucleus was diminished but persisted as a narrow band adjacent to the postacrosomal complex. While the edge regions of the acrosome remained as narrow bands, the central region started to enlarge and usually contained an electron lucent vesicle. Prominent Sertoli cell spurs extended from the edges of the acrosome and similar electron-dense material appeared in the Sertoli cell cytoplasm adjacent to the surface of the acrosome. Mitochondria were conspicuous in the Sertoli cell cytoplasm near the acrosome. Other spermatid organelles were similar to those in step 8.

Step 10 spermatids (*Fig. 10*). The nuclei of stage 10 spermatids had achieved the basic shape of the spermatozoon, with a large anterior portion and a narrow tapered posterior. The cross section of the anterior part was roughly triangular in shape, while at the point of tail insertion the nucleus had a more square cross section. The nuclear membrane of the future ventral surface (tail insertion side) of the head was separated from the condensed chromatin and the postacrosomal complex was evident adjacent to the posterior end of the nucleus. The acrosome covered the whole dorsal surface of the nucleus. In the central section of the acrosome the electron lucent vesicle was replaced by a subacrosomal space. The Sertoli cell spurs extended further from the spermatid and

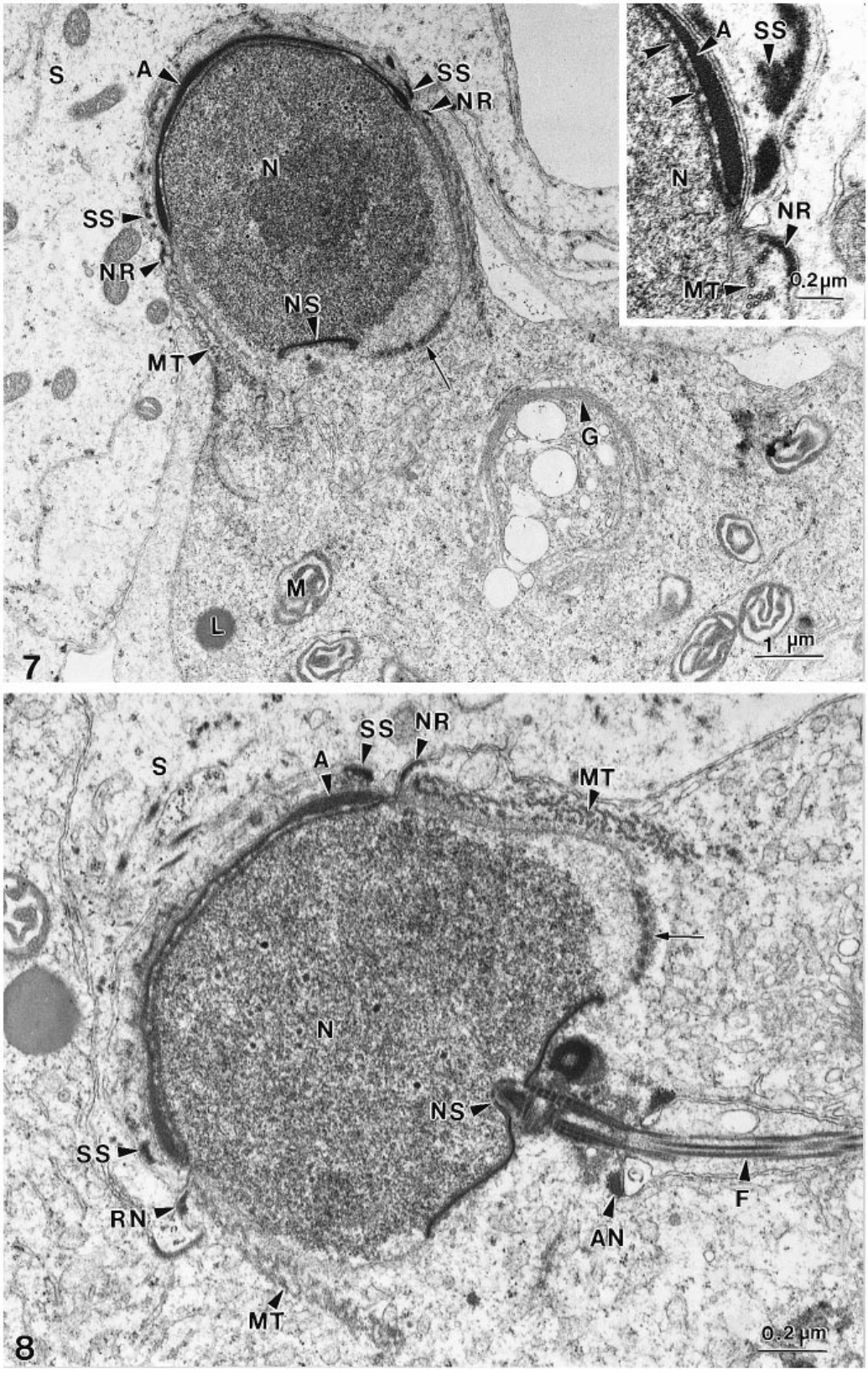

Fig. 7. Longitudinal section of a step 7 spermatid of the tammar wallaby. The postacrosomal complex (arrow) is seen on the nuclear membrane next to the nuclear socket (NS). The nuclear ring (NR) and the Sertoli cell spurs (SS) appear on the edge of the acrosome (A). The acrosome (A) covers the anterior end of the nucleus. Electron-dense granules (arrowheads in the inset) are located radially in a transparent area of the acrosome. A set of circular microtubules of the manchette (MT) appears on the lateral sides of the nucleus (N). Mitochondria (M) and Golgi bodies (G) have moved to the posterior end of the spermatid. L, Lipid droplet.

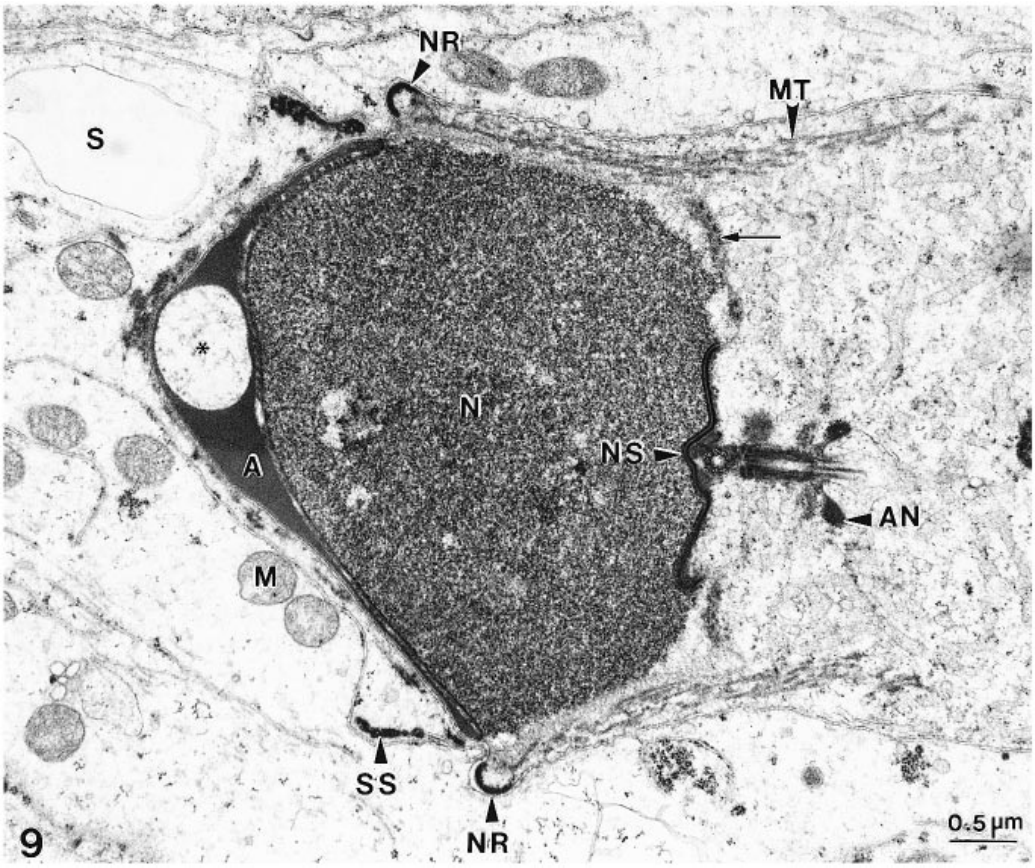

Fig. 9. Electron micrograph of a step 9 spermatid of the tammar wallaby. The nucleus (N) has started to turn into a cone shape. The central section of the acrosome (A) is thickened, and contains an electron lucent vesicle (*). Mitochondria (M) of the Sertoli cell (S) are aggregated in the area close to the acrosome. Sertoli cell spurs (SS) extend from the edge of the acrosome. AN, annulus; MT, microtubules of the manchette; NR, nuclear ring; NS, nuclear socket; arrow, postacrosome complex.

connected with the conspicuous electron-dense material in the Sertoli cell above the acrosome. The manchette had an unusually complex appearance. One set of manchette microtubules associated with the anterior ventral surface of the forming head ran parallel to the long axis of the spermatid (longitudinal microtubules; Fig. 10). A second set associated with the posterior extremity of the head ran perpendicular to the long axis of the spermatid (circular microtubules; Fig. 10). The unusual complexity of the manchette was seen in cross sections through the middle of the head (Fig. 10*b*), where circular and longitudinal microtubules lay on either side of the head. Other spermatid organelles were the same as in the previous step.

Step 11 spermatids (*Fig. 11*). The nuclear shaping process reached its final stage in step 11 spermatids. The nucleus had became an elongate arrowhead, and contained highly condensed chromatin. Viewed in longitudinal section, the flagellum was oriented at approximately 60° to the long axis of the nucleus. The acrosome covered the whole dorsal length of the nucleus, and at the anterior end extended beyond the nucleus as lateral projections. The subacrosomal space was much enlarged and extended from the anterior end of the nucleus to midway along its length. As a result, the anterior end of the acrosome did not contact the nucleus. The postacrosomal complex had moved along the ventral surface of the nucleus towards its posterior aspect. The nuclear ring continued to delineate the limit of the acrosome on the nuclear surface. Sertoli cell spurs now encircled and engulfed the part of the cytoplasm of Sertoli cell adjacent to the acrosome. The nuclear socket, the site of insertion of the tail into the nucleus, and the specialised neck or connecting piece of the flagellum

Fig. 8. Longitudinal section of a step 8 spermatid of the tammar wallaby. The nucleus (N) has a roughly square shape. The postacrosomal complex (arrow) appears next to the nuclear socket (NS) as a line of discontinuous electron-dense particles. The flagellum (F) is fully inserted into the nuclear socket (NS). A, acrosome; AN, annulus; MT, manchette microtubules; NR, nuclear ring; S, Sertoli cell cytoplasm; SS, Sertoli cell spurs.

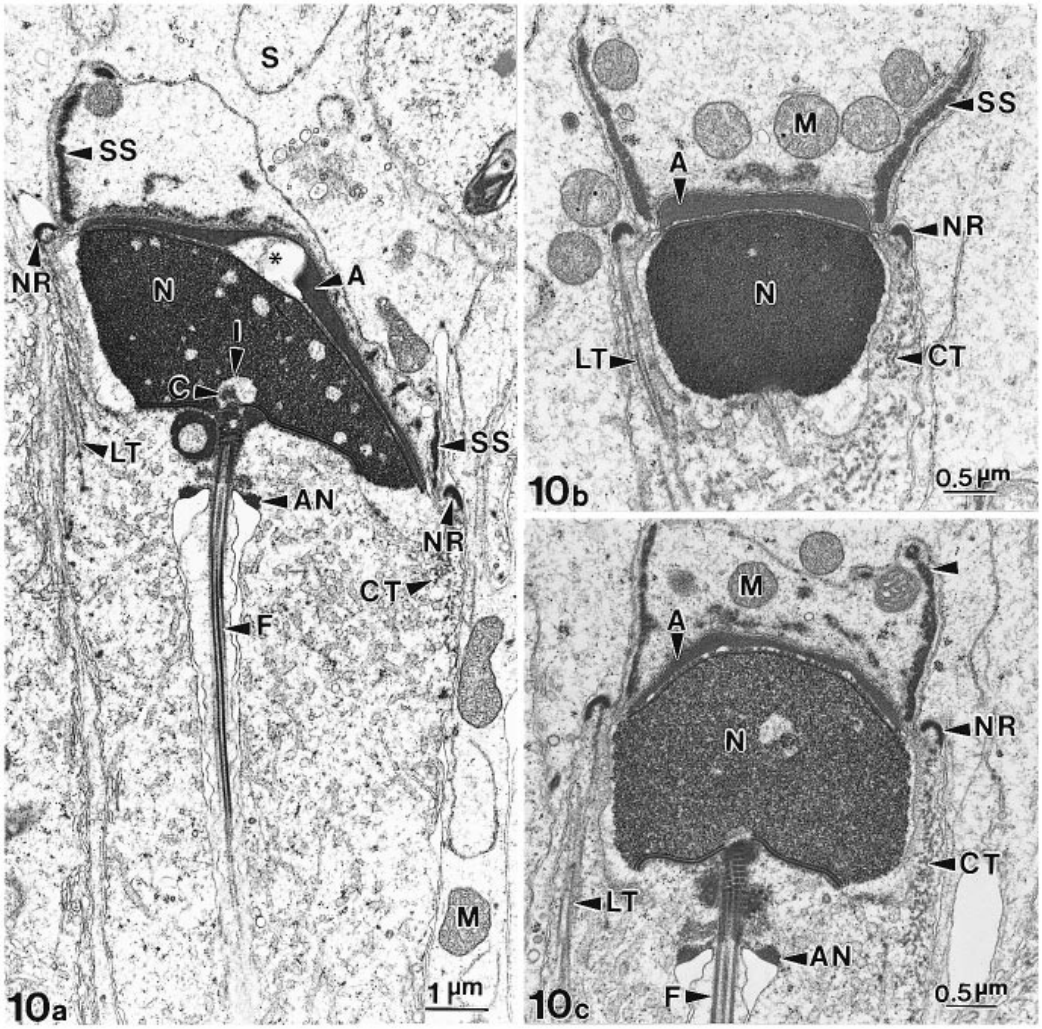

Fig. 10. Longitudinal and cross-sections of step 10 spermatids of the tammar wallaby. The nucleus (N) contains coarse chromatin granules and vesicles with lower electron density. The nucleus has a triangular shape in longitudinal section (*a*) with the acrosome (A) covering its entire anterior surface. A subacrosomal space (*) is seen in the central section of the acrosome (*a*, *b*). Microtubules of the manchette appear on both lateral sides of the nucleus (N), but run circularly on one side (CT) and longitudinally on the other (LT). The connecting piece (C) of the flagellum (F) and the implantation fossa (I) are forming (*a*, *c*). AN, annulus; M, mitochondria; NR, nuclear ring; SS, Sertoli cell spurs.

were fully formed. Conspicuous longitudinal microtubules of the manchette remained along the anterior ventral side of the nucleus. Microtubules were not evident at the posterior of the head.

Step 12 spermatids (*Fig. 12*). During this stage the acrosome began to be relocated forward on the nucleus. The anterior end of the acrosome protruded ahead of the nucleus, while the posterior end of the acrosome withdrew from the posterior end of the nucleus. A conspicuous nuclear ring circled the acrosome of step 12 spermatids. Step 12 also saw the initiation of midpiece formation. The axoneme of the distal centriole became elongated and mitochondria had begun to aggregate along the axoneme, between the neck and annulus. The fibrous sheath of the principal piece and an associated helical fibre network were evident at this stage.

Step 13 spermatids (*Fig. 13*). The nucleus had rotated to lie parallel to the flagellum and thus the step 13 spermatid had a streamlined shape. The

Fig. 11. Electron micrographs of step 11 spermatids of the tammar wallaby. The nucleus (N) is roughly spindle-shaped, contains highly condensed chromatin and is oriented nearly perpendicular to the sperm flagellum (F). A larger subacrosomal space (*) appears on the anterior end of the dorsal side of the nucleus. Sertoli cell spurs (SS) have engulfed part of Sertoli cell cytoplasm (S, inset) close to the acrosome (A). The nuclear ring (NR) remains on the edges of the acrosome. The longitudinal manchette (LT) persists but the circular manchette has disappeared. AN, annulus.

[*legend continues opposite*]

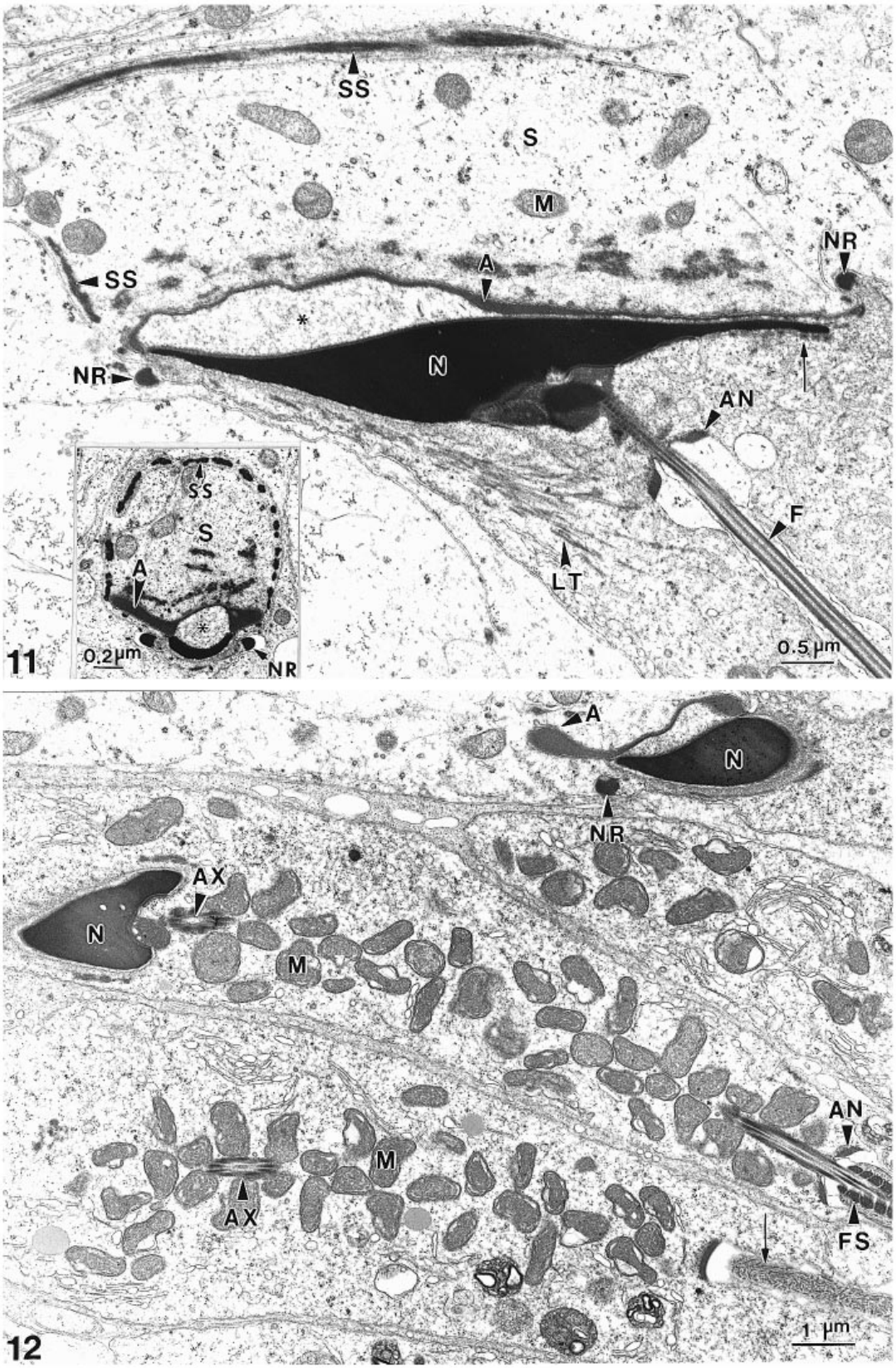

Fig. 12. Electron micrograph of step 12 spermatids of the tammar wallaby. The acrosome extension (A) stretches out of the anterior end of the nucleus (N), the nuclear ring (NR) remaining on the edge of the acrosome. Mitochondria (M) are gathered around the axoneme (AX) between the neck and the annulus (AN) to form the midpiece of the sperm. The fibre sheath (FS) is present in the principal piece, and is covered by a layer of helical fibre network (arrow).

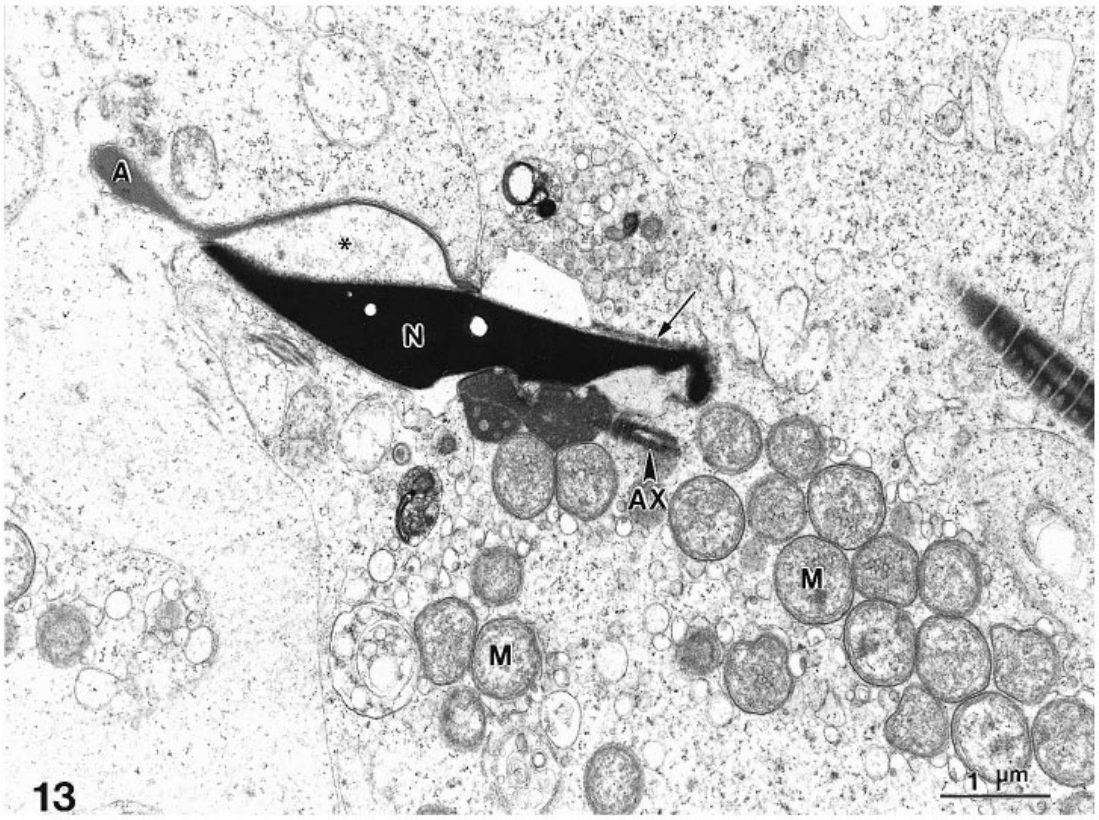

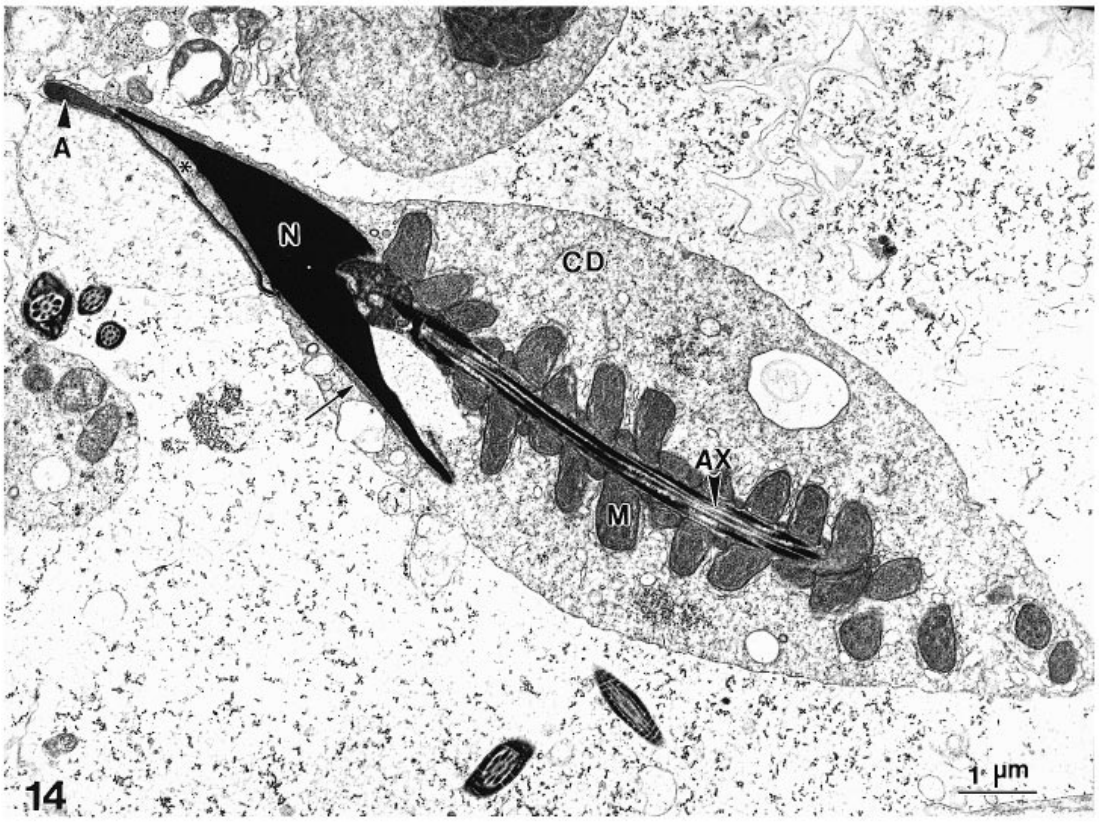

Fig. 13. Longitudinal section of a step 13 spermatid of the tammar wallaby. The nucleus is oriented parallel to the axoneme of the flagellum (AX) at this stage. The postacrosomal complex (arrow) has moved up to the dorsal side of the nucleus (N) close to the posterior end of the acrosome (A). The subacrosomal space (*) has persisted in the anterior end of the nucleus. Mitochondria (M) have accumulated in the midpiece area.

Fig. 14. Longitudinal section of a step 14 spermatid of the tammar wallaby. The nucleus is streamlined in the long axis of the spermatid. The subacrosomal space (*) is smaller. The mitochondria (M) completely surround the axoneme (AX) of the midpiece. A cytoplasmic droplet (CD) is located behind the nucleus at the anterior end of the midpiece.

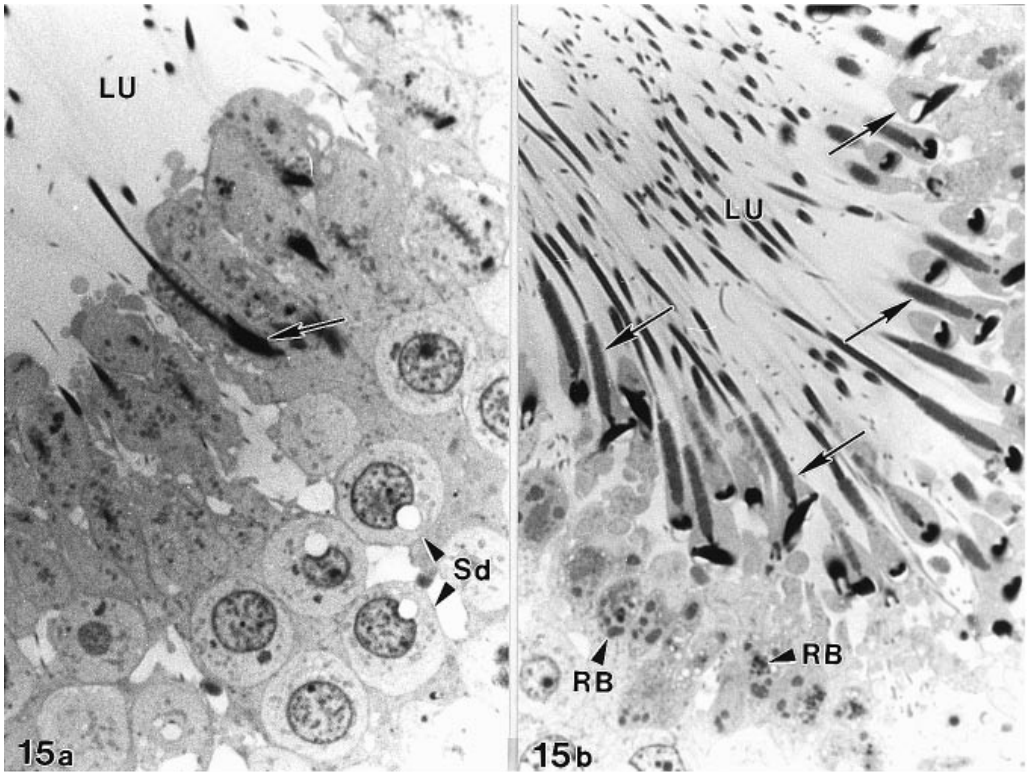

Fig. 15. Light micrographs of the luminal region of the seminiferous epithelium of the tammar wallaby. (*a*) Mature (step 14) spermatid (arrow) just before release into the lumen (LU) of the seminiferous tubule. Note the streamlined shape of the head. (*b*) Multiple wallaby spermatozoa (arrows) immediately after release from the seminiferous epithelium; the residual bodies (RB) are retained in the cytoplasm of Sertoli cells. Note that the heads of the released spermatozoa are rotated perpendicular to the tail, so that the spermatozoa have a T shape. Sd, young (step 4) spermatids.

anterior relocation of the acrosome continued, with the posterior end of the acrosome coming to lie midway along the dorsal side of the nucleus. Despite this forward movement, the large subacrosomal space remained located above the concavity on the anterior dorsal side of the nucleus. The postacrosomal complex was now located on the dorsal surface of the nucleus, but at its posterior extremity. Aggregation of mitochondria in the midpiece was marked.

Step 14 spermatids (*Fig. 14*). The subacrosomal space was markedly reduced and the acrosome was a thin sheet on the anterior end of the nucleus with an anterior projecting extension. The mitochondrial sheath of the midpieces was well formed, and the mitochondria had electron-dense matrices. The posterior head and midpiece were surrounded by an elongate cytoplasmic droplet which projected into the lumen of the seminiferous tubule. This was the final stage recognised before spermiation.

Spermiation

Streamlined step 14 spermatids with the head parallel to the flagellum (see Fig. 15*a*) were found in the top layer of the seminiferous epithelium. However, spermatozoa in the process of being released into the lumen of the seminiferous tubule possessed a 'T' or hammer shape (see Fig. 15*b*), with the head at approximately 90° to the flagellum. This orientation was similar to that seen in early spermatids.

During the final stages of spermatid-seminiferous tubule association the nucleus and tail had left the seminiferous epithelium but the acrosomal extensions remained embedded in the cytoplasm of the Sertoli cell (see Figs 16*a*, 17*a*). A fragment of Sertoli cell cytoplasm remained with the released spermatozoon and enclosed within the extensions of the acrosome (Figs 16*b*, 17*b*, 18*b*). The anterior extension of the acrosome was the last part of the spermatid to be released from the seminiferous epithelium (see Fig. 17*b*).

The 3-dimensional structure of the acrosome at spermiation was complex. Scanning electron micrographs indicated that the anterior and lateral extensions of the acrosome seen in transmission micrographs formed a posterior facing 'scoop-like' shape on the head of the testicular spermatozoa (Fig. 18*a*, *b*). As most of the cytoplasm of the spermatid was shed as residual bodies retained in the cytoplasm of the Sertoli cell (Fig. 19), the spermatozoon retained

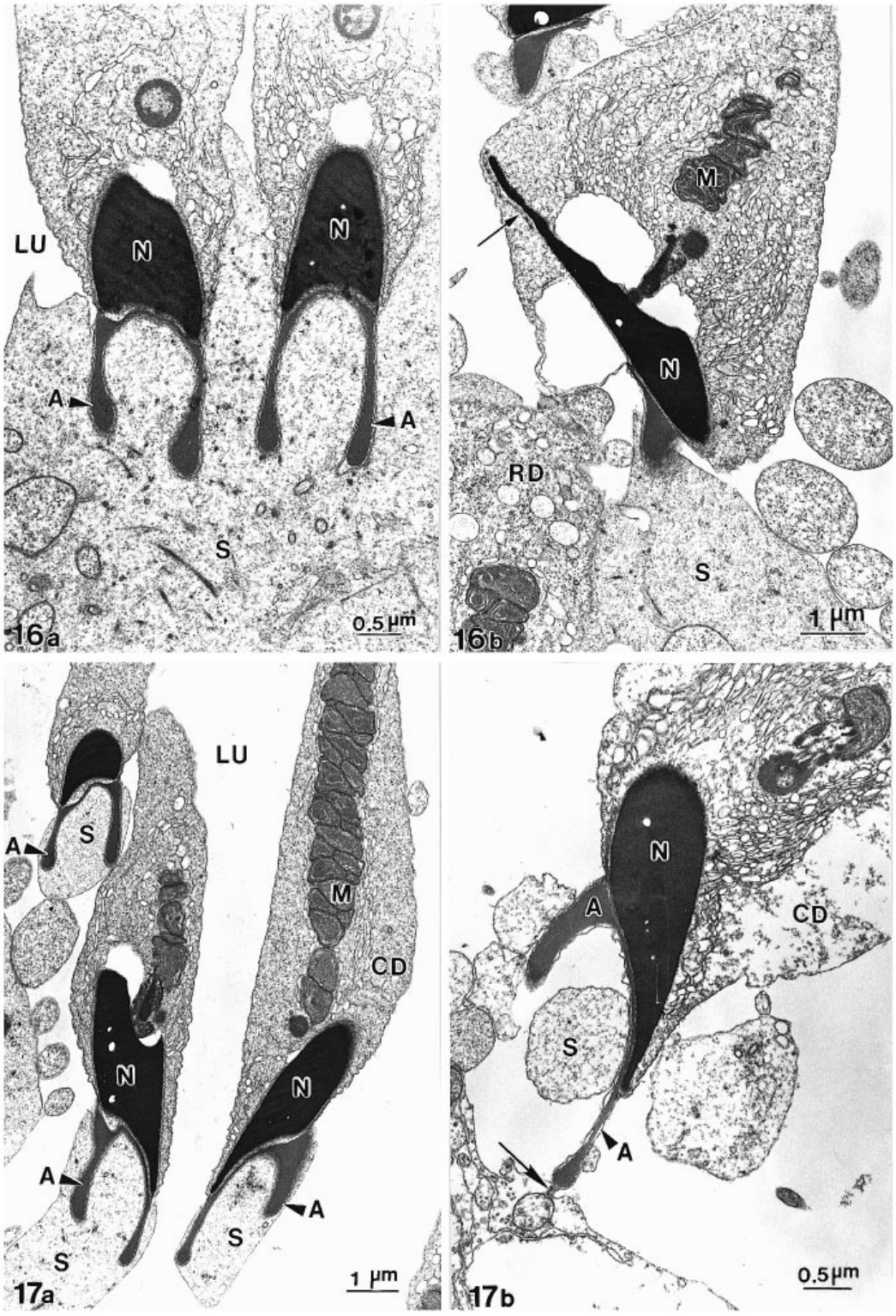

Fig. 16. Electron micrographs showing the mature spermatids being released from the seminiferous epithelium of the tammar wallaby. (*a*) The lateral extension of the acrosome (A) is still embedded in the Sertoli cell cytoplasm (S) when the tail and midpiece of the sperm are free from the seminiferous epithelium. LU, lumen. (*b*) Spermatozoa just before release into the lumen of the seminiferous tubule. The acrosome retains some parts of the Sertoli cell cytoplasm (S) with its lateral extension. M, mitochondria; N, nucleus; RD, residual body.

Fig. 17. Electron micrographs of the spermatids of the tammar wallaby. (*a*) Shows a whole spermatozoon lying free from the seminiferous epithelium, while the anterior end of the acrosome is still embedded in the cytoplasm of the Sertoli cell (S). The nucleus (N) is perpendicular to the axoneme of the midpiece. (*b*) Shows that the anterior end of the acrosome (A) is the last contact area (arrow) between the spermatid and the Sertoli cell. A drop of Sertoli cell cytoplasm (S) is engulfed within the acrosome (A). CD, cytoplasm droplet; LU, lumen; M, mitochondria; N, nucleus.

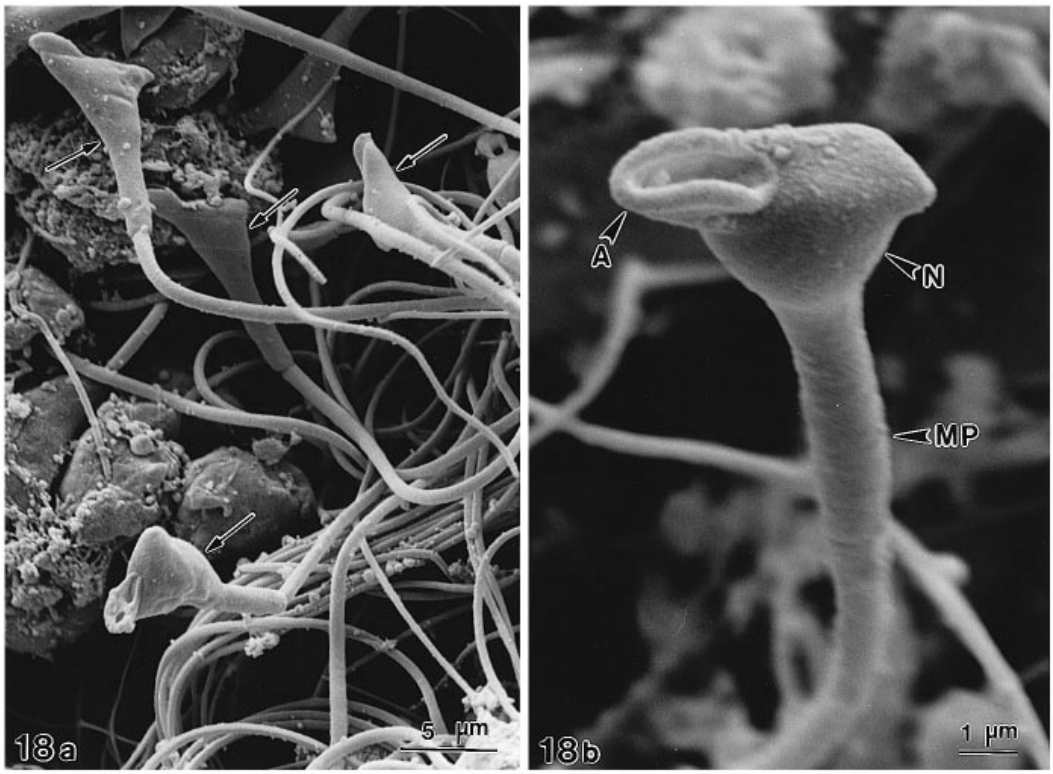

Fig. 18. Scanning electron micrographs of spermatozoa in the lumen of the seminiferous tubule of the tammar wallaby. (*a*) Spermatozoa (arrows) with roughly T-shaped heads in the lumen of the seminiferous tubule. (*b*) Acrosome with a 'scoop' shape on the anterior end of the nucleus (N), and containing a drop of Sertoli cell cytoplasm within the fold of the acrosome. MP, midpiece.

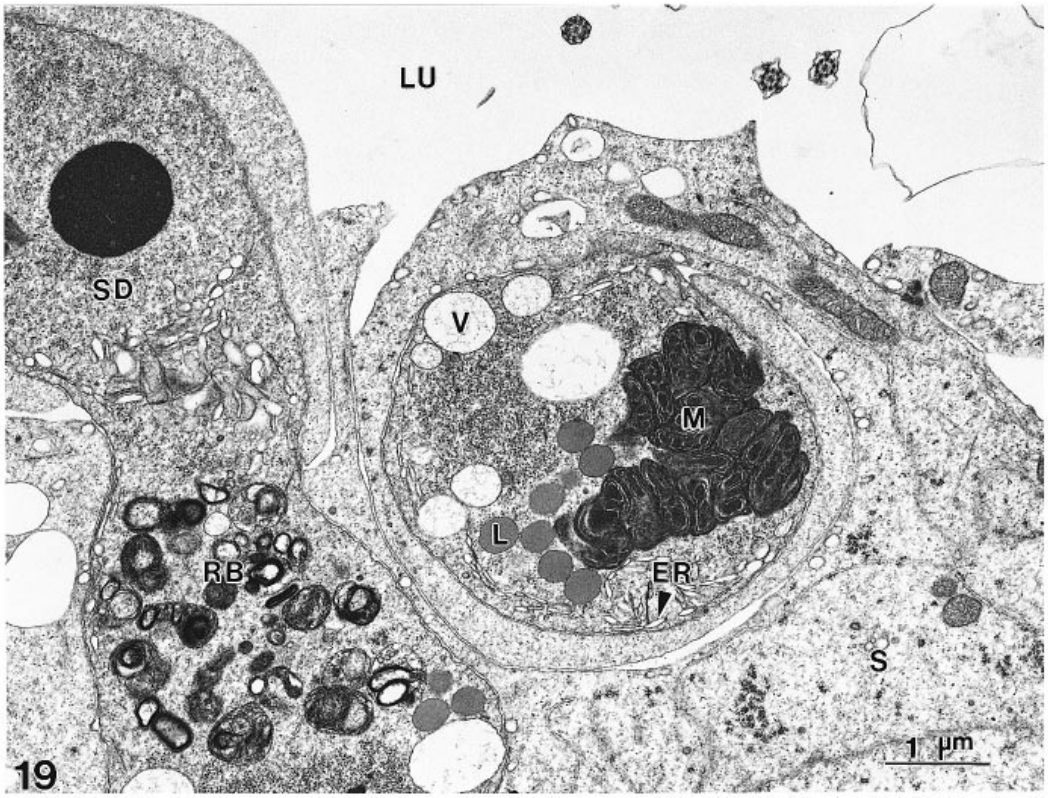

Fig. 19. Electron micrograph showing that a residual body (RB) was shed in the cytoplasm of the Sertoli cell (S) by a spermatid (SD) which was being released into the lumen of the seminiferous tubule (LU). The residual bodies contain mitochondria (M), endoplasmic reticulum (ER), membrane-bound vesicles (V) and lipid droplets (L).

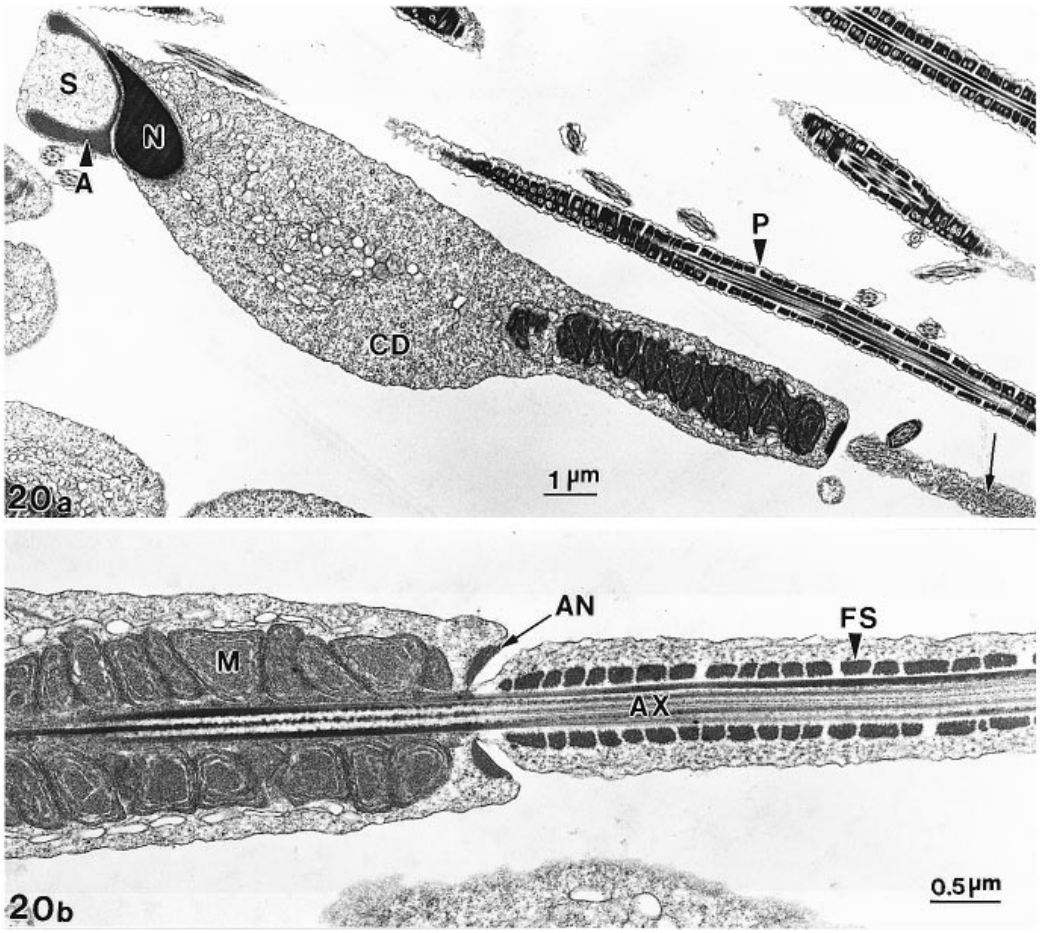

Fig. 20. Longitudinal sections of the tammar wallaby spermatozoa in the lumen of the seminiferous tubule. (*a*) Shows that the acrosome (A) has engulfed a patch of Sertoli cell cytoplasm (S) within the lateral extensions of the acrosome. The cytoplasm droplet (CD) is located on the anterior end of the midpiece, next to the nucleus (N). The principal piece (P) is covered by the fibre network (arrow). (*b*) Shows the arrangement of mitochondria (M), annulus (AN) and fibre-sheath (FS) around the axoneme (AX) at the conjunction of the midpiece and the principal piece. Note that no fibre network appears beneath the cytoplasmic membrane of the midpiece in the testicular spermatozoon.

some as a cytoplasm droplet on its neck region when it was released into the lumen of the seminiferous tubule (Fig. 20*a*). The fibre network found beneath the cytoplasmic membrane of the midpiece of the ejaculated sperm did not occur in the testicular spermatozoa (Fig. 20*b*). The structure of the principal piece was fully formed and had no obvious morphological difference from that of the epididymal and ejaculated spermatozoa (unpublished observation).

DISCUSSION

Ultrastructural observations in the tammar wallaby (*Macropus eugenii*) confirmed that though the main events are generally similar, the process of the differentiation of the spermatid in marsupials is notably different and relatively more complex than that in most studied eutherian mammals and birds. For example, one of the most distinctive elements in the sperm head of marsupials is the insertion of the tail. In almost all marsupial species, the connection piece of the tail does not adjoin the posterior end of the nucleus as is usually the case in eutherian mammals, but inserts into a fossa in the midventral face of the nucleus (Bedford, 1991). In the late stage of spermiogenesis of the tammar wallaby, the angle of the tail insertion into the nucleus actually forms a T configuration between nucleus and tail twice (from T-shape in step 10 spermatids to streamline in step 14 spermatids, and then back to T-shape in the testicular spermatozoa). A similar pattern of head rotation has been found in other marsupial species, such as in the bandicoot (*Perameles nasuta*; Sapsford et al. 1969*a*, *b*) and brush-tailed possum (*Trichosurus vulpecula*; Harding et al. 1976). In fact, the wallaby sperm head will repeat the rotations twice more, once during spermatozoon transit through the epididymis and the other in the female reproductive tract (unpublished observation). Some unique figures occurring during the spermiogenesis in other marsupial species, such as

the presence of Sertoli cell spurs, the nuclear ring and the subacrosomal space, were also found in the tammar wallaby.

One of the important new findings of the present study is the development of the postacrosome complex (PAC), a structure first evident on the nuclear membrane of the step 7 spermatid (see Fig. 7). A similar structure is present in published micrographs of the woolly opossum (*Caluromys philander*; Phillips, 1970). In cross sections of the nucleus, the PAC first appears in the wallaby spermatid as a line of electron dense material on the nuclear membrane, and close to the flagellum insertion (nuclear socket). Subsequently it becomes a discontinuous line of electron-dense particles (see Fig. 8), and migrates from the ventral to the dorsal side of the nucleus and finally to the area just behind the posterior end of the acrosome (see Figs 13, 14).

Both in amphibians (Picheral & Charbonneau, 1982) and birds (Okamura & Nishiyama, 1978) sperm–egg fusion occurs at the inner acrosomal membrane of the sperm head. In eutherian mammals ultrastructural studies show that the sperm plasmalemma over the equatorial segment of the acrosome (retained following the acrosome reaction) fuses with the oolemma (Moore & Bedford, 1978; Bedford et al. 1979). In marsupial spermatozoa, however, the exhibition of an equatorial segment structure in the sperm head is uncertain (Temple-Smith, 1987; Rodger, 1996). Investigation of sperm–egg fusion has been carried out in very few marsupial species, and 2 modes of this important phase have been suggested. From studies in the Virginian opossum (*Didelphis virginiana*), Rodger & Bedford (1982) favoured the view that sperm-egg fusion occurred over the inner acrosome membrane. However, Taggart et al. (1993) found that in the grey short-tailed opossum (*Monodelphis domestica*) the fusion first appeared over the marginal acrosomal region in a manner reminiscent of eutherian fertilisation. The PAC found in the tammar wallaby was closely located to the fusion site proposed for *Monodelphis domestica*, and its special discontinuous type of structure was remarkably different from the rest of the nuclear membrane. The PAC and its possible role both in American and Australian marsupials requires detailed examination.

The development of the acrosome in the tammar wallaby follows the general pattern described for other marsupial species (Harding et al. 1979). The present study confirmed that the acrosome of the tammar wallaby arises from the fusion of several membrane-bound vesicles into a large electron-lucent acrosomal vacuole (Fig. 3). The electron-lucent appearance of the acrosomal vacuole was similar to that found in the brush-tailed possum (Harding et al. 1976), the bandicoot (*Perameles nasuta*; Sapsford et al. 1969*a*, *b*) and other marsupial species (Harding et al. 1979). However, it is very different from that in most eutherian mammals, in which a granular acrosomal vacuole is found at an early stage of spermatogenesis (Bloom & Fawcett, 1975). The electron-lucent acrosomal vacuole was also found in the monotremes (the platypus, *Ornithorhynchus anatinus*; Lin & Jones, 1994).

When the mature tammar wallaby spermatid is released into the lumen of the seminiferous tubule to become a spermatozoon, its acrosome is a scoop-shaped sheet of folding tissue (Fig. 18*b*). The shape was completely different to the acrosome of ejaculated spermatozoa, which is a compact button lodged in a depression on the dorsal side of the nucleus (Cummins, 1979; Setiadi et al. 1997). A scoop shape of the acrosome was also found on the testicular spermatozoa of the brushtail possum (unpublished observation). Similar complex posttesticular condensation of the acrosomal maturation has been found in many Australian marsupial species (Harding et al. 1983).

Another distinct immature feature was found in the midpiece of the testicular spermatozoa. In mature wallaby spermatozoa, immediately beneath the cytoplasmic membrane of the midpiece there is a set of helically wound fibres which completely surround the midpiece from the posterior end of the nucleus to the annulus region (unpublished observation). However, in the midpiece of the testicular spermatozoa this set of fibres is absent (see Fig. 20*b*). A similar fibre structure was found in the brushtail possum (Temple-Smith & Bedford, 1976) and other marsupial species (Harding et al. 1976, 1984), and was designated as the midpiece fibre network. In the possum, the midpiece fibre network started to form in the region of the distal caput epididymis, and fully formed after the spermatozoa passed through the proximal cauda epididymis (Temple-Smith & Bedford, 1976). The time frame of the formation of this fibre network in the tammar wallaby needs to be determined by further studies.

Manchette microtubules are a common feature found during spermiogenesis in all mammals and birds studied to date (see review by Fawcett et al. 1971; Guraya, 1987; Jones & Lin, 1993), and marsupial species are no exception (Harding et al. 1979). However, in most eutherian mammals and birds, the manchette consists of 2 distinctive sets of microtubules: the circular and the longitudinal

manchette. The circular manchette occurs in the early stages of spermiogenesis and is arranged in a plane perpendicular to the longitudinal axis of the nucleus, while the longitudinal manchette replaces the circular manchette in late stages of spermiogenesis, and appears as an array of almost straight microtubules lying parallel to the longitudinal axis of the nucleus. In marsupials, it is very difficult to identify those 2 sets of manchette microtubules. Although the manchette tubules are seemingly arranged as a set of circular manchette microtubules in early round wallaby spermatids (Figs 6, 7), in late spermatids some of the manchette microtubules run circularly on one side of the nucleus, while the others run longitudinally on the opposite side of the nucleus. It is unknown whether there were 2 separate sets of microtubules occurring at different times, or one set of tubules which were arranged in different directions because of the unique shape and orientation of the sperm nucleus in marsupials. Although the significance of the manchette during nuclear elongation of mammalian spermatids is still debatable (see review by Fawcett et al. 1971; Guraya, 1987), work on birds (Nagano, 1962; Okamura & Nishiyama, 1976; Gunawardana & Scott, 1977; Lin & Jones, 1993; Lin et al. 1995) suggests that the microtubules of the manchette play an important role in nuclear morphogenesis, since the development of microtubules closely coincides with the process. The unusual organisation of the manchette microtubules in marsupial spermatid differentiation would suggest a role in the shaping of the sperm head.

During the development of the acrosome, a subacrosomal space (a very common feature found in most marsupials) occurred on the dorsal surface of the wallaby spermatids (Fig. 11). The mechanism of the formation of this special structure is not understood. Based on information obtained from the brush-tail possum and honey possum, Harding et al. (1976, 1984) suggested that a contraction of the nuclear ring (another special feature only found in marsupials) caused the constriction of the acrosomal material into a reduced area bounded by the ring, and brings about the formation of the subacrosomal space. However, no evidence to support this suggestion was found in the tammar wallaby. The subacrosomal space in the wallaby spermatids appeared to originate from an electron-lucent vesicle within the matrix of the acrosome (Figs 9, 10*a*). When the subacrosomal space was fully formed, the acrosomal material still covered the whole dorsal side of the nucleus, and the nuclear ring had not contracted and was still located outside the area of the nucleus (see Fig. 11).

The Sertoli cell spur is another special feature found during marsupial spermiogenesis. In the later stages of spermiogenesis, the Sertoli cell cytoplasm in the region of the developing acrosome was modified into electron-dense fibrous materials, and projected like spurs into the Sertoli cell cytoplasm. In the tammar wallaby Sertoli cell spurs first occurred in step 7 spermatids (Fig. 7), developed fully in the step 11 spermatid (Fig. 11) and disappeared in step 12 spermatids (Fig. 12). When fully developed, the spur projections fused together to form a sheet of electron-dense material which engulfed part of Sertoli cell cytoplasm in the acrosome region (see Fig. 11). To name this structure of modified Sertoli cell cytoplasm a spur does not adequately reflect its shape; Sertoli cell sheet may be more appropriate.

Some significant differences in spermiation of the tammar wallaby have been identified in this study. First, there is a difference in the elimination of spermatid cytoplasm destined to form the residual body. In mammals, the excess cytoplasm accumulates around the neck of spermatids, and during spermiation a long, slender stalk joins the spermatid to the putative residual body held within the Sertoli cell cytoplasm (see Fawcett & Phillips, 1969). When the connecting stalk is broken, the proximal end retracts to form the cytoplasmic droplet around the neck of the spermatozoon (Fawcett & Phillips, 1969; Russell & Clermont, 1976; Holstein & Roosen-Runge, 1981). In the tammar wallaby, just before spermiation the spermatid had a streamlined head-tail orientation and the excess spermatid cytoplasm accumulated in the anterior end of the head near the acrosome (see Fig. 15*a*). The spermatid was separated from the putative residual body by a short bridge of cytoplasm (Fig. 19). Immediately after the spermatid was released from the seminiferous epithelium, its head rotated through 90° into a T shape. Consequently, the anterior extension of the acrosome was the final point of contact with the seminiferous epithelium. A drop of Sertoli cell cytoplasm was held in the scoop shape of the acrosome of spermatozoa released to the lumen of the seminiferous tubule (see Figs 17*b*, 18*b*). The fate of this drop of Sertoli cell cytoplasm and how it relates to the transformation of the acrosome in the epididymis need to be examined in further studies.

REFERENCES

Bedford JM (1991) The coevolution of mammalian gametes. In *A Comparative Overview of Mammalian Fertilization* (ed. Dunbar BS, O'Rand MG), pp. 3–35. New York: Plenum Press.

Bedford JM, Moore HDM, Franklin LE (1979) Significance of the equatorial segment of the acrosome of the spermatozoon in eutherian mammals. *Experimental Cell Research* **119**, 119–126.

Bloom W, Fawcett DW (1975) Spermatogenesis. In *A Textbook of Histology* (ed. Bloom W, Fawcett DW), pp. 819–833, Philadelphia: W. B. Saunders.

Cleland KW (1956) Acrosome formation in bandicoot spermiogenesis. *Nature* **177**, 387–388.

Cleland KW, Lord Rothschild (1959) The bandicoot spermatozoon: an electron microscope study of the tail. *Proceedings of Royal Society of London* (*Biology*) **150**, 24–42.

Cummins JM (1979) Sperm maturation in the epididymis of the tammar wallaby, *Macropus eugenii*. *Proceedings of the Australian Mammal Society* (abstract) pp. 16.

Fawcett DW, Phillips DM (1969) Observation on the release of spermatozoa and on changes in the head during passage through the epididymis. *Journal of Reproduction and Fertility*, Suppl. **6**, 405–418.

Fawcett DW, Anderson WA, Phillips DM (1971) Morphogenetic factors influencing the shape of the sperm head. *Developmental Biology* **26**, 220–251.

Gunawardana VK, Scott MGAD (1977) Ultrastructural studies on the differentiation of spermatids in the domestic fowl. *Journal of Anatomy* **124**, 741–755.

Guraya SS (1987) *Biology of Spermatogenesis and Spermatozoa in Mammals*, pp. 142–148. Berlin: Springer.

Harding HR, Carrick FN, Shorey CD (1976) Spermiogenesis in the brush-tailed possum, *Trichosurus vulpecula* (Marsupialia) – the development of the acrosome. *Cell and Tissue Research* **171**, 75–90.

Harding HR, Carrick FN, Shorey CD (1979) Special features of sperm structure and function in marsupials. In *The Spermatozoon: Maturation, Motility, Surface Properties and Comparative Aspects* (ed. Fawcett DW, Bedford JM), pp. 289–303. Baltimore-Munich: Urban and Schwarzenberg.

Harding HR, Woolley PA, Shorey CD, Carrick FN (1982) Sperm ultrastructure, spermiogenesis and epididymal sperm maturation in dasyurid marsupials: phylogenetic implications. In *Carnivorous Marsupials* (ed. Archer M), pp. 659–673, Sydney: Royal Zoological Society of New South Wales.

Harding HR, Carrick FN, Shorey CD (1983) Acrosome development during spermiogenesis and epididymal sperm maturation in Australian marsupials. In *The Sperm Cell* (ed. Andre J), pp. 411–444. The Hague: Martinus Nijhoff.

Harding HR, Carrick FN, Shorey CD (1984) Sperm ultrastructure and development in the honey possum, *Tarsipes rostratus*. In *Possums and Gliders* (ed. Smith AP, Hume ID), pp. 451–456. Sydney: Australian Mammal Society.

Holstein AF, Roosen-Runge EC (1981) *Atlas of Human Spermatogenesis*, pp. 33–57. Berlin: Grosse.

Hughes RL (1965) Comparative morphology of spermatozoa from five marsupial families. *Australian Journal of Zoology* **13**, 533–543.

Jones RC, Lin M (1993) Spermatogenesis in birds. In *Oxford Reviews of Reproductive Biology*, vol. 15 (ed. Milligan SR), pp. 233–264. Oxford: Oxford University Press.

Kim JW, Harding HR, Shorey CD (1987) Electron-microscopic studies on the spermiogenesis and spermatozoa of the allied rock wallaby (*Petrogale assimilis*). *Korean Journal of Electron Microscopy* **17**, 1–15.

Lin M, Jones RC (1993) Spermiogenesis and spermiation in the Japanese quail (*Coturnix coturnix japonica*). *Journal of Anatomy* **183**, 525–535

Lin M, Jones RC (1994) Spermiogenesis and spermiation in the platypus, *Ornithorhynchus anatinus*. *Eighth European Workshop on Molecular and Cellular Endocrinology of the Testis*, pp. 82. Belgium: De Panne.

Lin M, Thorne MH, Martin ICA, Sheldon RL, Jones RC (1995) Electron microscopy of the seminiferous epithelium in the triploid (ZZ and ZZW) fowl, *Gallus domesticus*. *Journal of Anatomy* **186**, 563–576.

Moore HDM, Bedford JM (1978) Ultrastructure of the equatorial segment of hamster spermatozoa during penetration of oocytes. *Journal of Ultrastructure Research* **62**, 110–117.

Nagano T (1962) Observations on the fine structure of developing spermatid in the domestic chicken. *Journal of Cell Biology* **14**, 193–205.

Okamura F, Nishiyama H (1976) The early development of the tail and the transformation of the shape of the nucleus of the spermatid of the domestic fowl, *Gallus domesticus*. *Cell and Tissue Research* **169**, 345–359.

Okamura F, Nishiyama H (1978) Penetration of the spermatozoon into the ovum and transformation of the sperm nucleus into the male pronucleus in the domestic fowl, *Gallus gallus*. *Cell and Tissue Research* **190**, 89–98.

Oko RJ (1995) Developmental expression and possible role of perinuclear theca proteins of mammalian spermatozoa. In *Seventh International Symposium on Spermatology: Plenary Papers*. *Reproduction, Fertility and Development* **7**, 119–140.

Phillips DM (1970) Development of spermatozoa in the wooly opossum with special reference to the shaping of the sperm head. *Journal of Ultrastructure Research* **33**, 369–380.

Picheral B, Charbonneau M (1982) Anuran fertilization: a morphological reinvestigation of some early events. *Journal of Ultrastructure Research* **81**, 306–321.

Rodger JC (1991) Fertilization of marsupials. In *A Comparative Overview of Mammalian Fertilization* (ed. Bonnie S, Michael G), pp. 117–135. New York: O'Rand Plenum.

Rodger JC (1996) Towards fertility management of marsupials – a case study. *Fourth International Conference on Fertility Control for Wildlife Management*, pp. 46–47. Australia: Great Keppel Island, Queensland.

Rodger JC, Bedford JM (1982) Separation of sperm pairs and sperm-egg interactions in the opossum, *Didelphis virginiana*. *Journal of Reproduction and Fertility* **64**, 171–179.

Russell L, Clermont Y (1976) Anchoring device between Sertoli cells and late spermatids in rat seminiferous tubules. *Anatomical Record* **185**, 259–278.

Sapsford CS, Rae CA, Cleland KW (1969*a*) The fate of residual bodies and degenerating germ cells and the lipid dydle in Sertoli cells in the bandicoot *Perameles nasuta Geoffroy* (Marsupialia). *Australian Journal of Zoology* **17**, 729–753.

Sapsford CS, Rae CA, Cleland KW (1969*b*) Ultrastructural studies on maturing spermatids and on Sertoli cells in the bandicoot *Perameles nasuta Geoffroy* (Marsupialia). *Australian Journal of Zoology* **17**, 195–292.

Sapsford CS, Rae CA, Cleland KW (1970) Ultrastructural studies on the development and form of the principal piece sheath of the bandicoot spermatozoon. *Australian Journal of Zoology* **18**, 21–48.

Setchell BP (1978) Spermatogenesis. In *The Mammalian Testis* (ed. Finn CA), pp. 181–232. London: Paul Elek.

Setiadi D, Lin M, Rodger JC (1997) Post-testicular development of spermatozoa of the tammar wallaby (*Macropus eugenii*). *Journal of Anatomy* **190**, 275–288.

Taggart DA, O'Brien HP, Moore HDM (1993) Ultrastructural characteristics of in vivo and in vitro fertilization in the grey short-tailed opossum, *Monodelphis domestica*. *Anatomical Record* **237**, 21–37.

Temple-Smith P (1987) Sperm structure and marsupial phylogeny. In *Possums and Opossums: Studies in Evolution* (ed. Archer M), pp. 171–193. Sydney: Surrey Beatty and Royal Zoological Society of New South Wales.

Temple-Smith PD, Bedford JM (1976) The features of sperm maturation in the epididymis of a marsupial, the brushtailed possum *Trichosurus vulpecula*. *American Journal of Anatomy* **147**, 471–500.